Submicroscopic calcium signals as fundamental events of excitation–contraction coupling in guinea-pig cardiac myocytes

Peter Lipp and Ernst Niggli*

Department of Physiology, University of Bern, Bühlplatz 5, 3012 Bern, Switzerland

1. Subcellularly localized Ca^{2+} signals have been proposed to represent elementary events of cardiac Ca^{2+} signalling (Ca^{2+} sparks), whereby an individual sarcolemmal L-type Ca^{2+} channel locally controls opening of a single (or a few) Ca^{2+} release channels in the sarcoplasmic reticulum (SR).

2. To investigate directly the elementary nature of this Ca^{2+}-induced Ca^{2+} release mechanism we used flash photolysis of caged Ca^{2+} while simultaneously measuring the intracellular Ca^{2+} concentration ($[Ca^{2+}]_i$) with a laser-scanning confocal microscope.

3. Power spectral analysis of the confocal images performed in the spatial domain revealed that only Ca^{2+} signalling events involving the L-type Ca^{2+} channel pathway gave rise to Ca^{2+} sparks. In contrast, SR Ca^{2+} release triggered by photolytic $[Ca^{2+}]_i$ jumps resulted in Ca^{2+} transients that were always spatially homogeneous.

4. From these findings we conclude that the fundamental event of Ca^{2+} signalling in cardiac muscle may be smaller in size or amplitude than a Ca^{2+} spark.

5. We term this event a 'Ca^{2+} quark' possibly resulting from gating of a single SR Ca^{2+} release channel. It is proposed that concerted activation of several 'Ca^{2+} quarks' may be required for a Ca^{2+} spark. The 'Ca^{2+} quark' could also be the fundamental event in other cell types implementing a hierarchical Ca^{2+} signalling concept.

In cardiac muscle cells, the small Ca^{2+} trigger signal entering via voltage-dependent sarcolemmal (SL) Ca^{2+} channels is amplified several-fold by Ca^{2+}-induced Ca^{2+} release (CICR) from the sarcoplasmic reticulum (SR) via Ca^{2+} release channels (Fabiato, 1985; Näbauer, Callewaert, Cleemann & Morad, 1989; Niggli & Lederer, 1990). This process usually generates a graded Ca^{2+} response without being highly regenerative (i.e. the release is not all-or-none). Nevertheless, the same amplification system is also known to create incidentally subcellularly localized spontaneous Ca^{2+} release events (Ca^{2+} sparks) in resting cardiac myocytes (Hermsmeyer, Mason, Puga & Erne, 1991; Niggli & Lipp, 1992; Cheng, Lederer & Cannell, 1993; Lipp & Niggli, 1994*b*). Moreover, when the number of available SL Ca^{2+} channels is reduced with pharmacological inhibitors (e.g. verapamil), the usually homogeneous Ca^{2+} transient breaks down into Ca^{2+} sparks, indicating that the sparks can also be elicited via the regular Ca^{2+} signalling pathway (see Fig. 1*A* and Cannell, Cheng & Lederer, 1994; López-López, Shacklock, Balke & Wier, 1995). Based on their voltage dependence and kinetics these triggered Ca^{2+} sparks have been proposed to arise from the gating of a single (or a few) SR Ca^{2+} release channels (ryanodine receptors) under the local control of an SL Ca^{2+} channel (dihydropyridine receptor). However, the exact micro-architecture of the cellular membranes in the SL–SR junction (triad or diad) and the functional relationship of the channel proteins involved has remained elusive. For a complete understanding of the various forms of cardiac Ca^{2+} signalling, including excitation–contraction coupling (E–C coupling) and Ca^{2+} waves (Wier, Cannell, Berlin, Marban & Lederer, 1987), it is essential to understand how these channels interact with Ca^{2+} and with each other on the molecular level. Different designs are plausible. (i) There could indeed be a functional 1 : 1 coupling between SL Ca^{2+} channels and the juxtaposed SR Ca^{2+} release channels. (ii) SR channels could be morphologically clustered to form functional units controlled by a single SL Ca^{2+} channel (see Fig. 1*C*). (iii) The domain of elevated Ca^{2+} around the inner opening of a SL Ca^{2+} channel itself might determine and limit the size of the triggered spark, even if the SR Ca^{2+} channels were distributed homogeneously.

* To whom correspondence should be addressed.

This manuscript was accepted as a Short Paper for rapid publication.

Information about these different schemes is of critical importance for our understanding of the cardiac Ca^{2+} signalling pathways. In the present study we tried to narrow down these possibilities by combining laser-scanning confocal imaging of Ca^{2+} signals in voltage-clamped guinea-pig ventricular myocytes with flash photolysis of caged Ca^{2+}. This alliance of biophysical techniques bears the experimental capability of directly activating CICR without involving SL Ca^{2+} channels. Depending on the precise size and the signal-to-noise ratio of the fundamental SR Ca^{2+} release event, photolytic trigger signals with energies slightly above the trigger threshold for CICR would be expected to recruit only a few of these elements and thus make them discernible, analogous to the situation where only a few SL Ca^{2+} channels are active in the presence of a submaximal concentration of an inhibitor (Cannell *et al.* 1994).

METHODS

Cell isolation and experimental solutions

Guinea-pigs were killed by cervical dislocation after stunning. Ventricular myocytes were isolated enzymatically (Lipp & Niggli, 1994*a*). The whole-cell mode of the patch-clamp technique was used to measure membrane currents while the intracellular Ca^{2+} concentration ($[Ca^{2+}]_i$) was simultaneously monitored with a laser-scanning confocal microscope (MRC-600, BioRad, Glattbrugg, Switzerland), as described recently (Lipp, Lüscher & Niggli, 1996). The external solution contained (mM): NaCl, 140; KCl, 4; $CaCl_2$, 2; glucose, 10; Hepes, 10; CsCl, 2; 10 μM verapamil; the pH was adjusted to 7·4 with NaOH. The temperature range was 20–22 °C. The pipette was filled with (mM): caesium aspartate, 120; TEA-Cl_2, 20; Hepes, 20; NaCl, 10; K_2-ATP, 4; Na_4-DM-nitrophen, 1; $CaCl_2$, 0·25; reduced glutathione (GSH), 2; the pH was adjusted to 7·2 with CsOH. Either 100 μM fluo-3 or 66 μM fura-red and 33 μM fluo-3 were added. From a holding potential of −50 mV five to ten prepulses (to +50 mV; duration, 500 ms; frequency, 0·5 Hz) were applied to ensure (i) comparable loading of the SR and DM-nitrophen with Ca^{2+} and (ii) inhibition of the L-type Ca^{2+} current. Due to the affinity of DM-nitrophen for Mg^{2+} ($K_D \approx 5$ μM) we had to omit Mg^{2+} from the experimental solutions. An effect of Mg^{2+} on the Ca^{2+} sensitivity and adaptation of single ryanodine receptors has been described (Valdivia, Kaplan, Ellis-Davies & Lederer, 1995) that could underlie the slightly prolonged time course of the Ca^{2+} sparks in the present study in comparison with earlier reports (López-López *et al.* 1995).

Current and calcium measurements

Analysis of the images and the membrane currents was performed using a customized version of NIH Image (NIH, Bethesda, MD, USA) and Igor (Wavemetrics, Lake Oswego, OR, USA). The $[Ca^{2+}]_i$ traces were computed using two different techniques. When fluo-3 was the only Ca^{2+} indicator, a self-ratio method was applied with published calibration parameters assuming a resting $[Ca^{2+}]_i$ of 100 nM (Cheng *et al.* 1993). The fluo-3–fura-red ratio was calibrated according to an *in vivo* calibration described elsewhere (Lipp *et al.* 1996). Ratiometric line-scan images were derived with a pixel-by-pixel division of the fluo-3 image by the fura-red image. Scanning, the flash and the voltage clamp were synchronized by a custom-made electronic device that allowed microsecond timing. The set-up was controlled by a PowerPC 8100/100 (Apple) equipped with a data-acquisition board (NB-MIO-16) running software developed by us under LabView (both from National Instruments, Austin, TX, USA).

Digital image processing

Power spectra of the line-scans were computed using IDL software (Research Systems, Boulder, CO, USA). Raw line-scan images were Fourier transformed line by line (i.e. in the spatial domain). The calculated power spectra of all lines were arranged in the same order as the original line-scan image. To compensate for changes in fluorescence, the power of each frequency component (P_i) was normalized by division with the zero-frequency component (P_0) to obtain P_{norm} (Cheng *et al.* 1993). The power spectra were independent of the line-scan direction with respect to the cell axis. Normalized power was simultaneously coded as height and colour of a 3-D surface.

The resolution of the confocal microscope is not adequate to spatially resolve nanoscopic Ca^{2+} signals; thus the apparent size of recorded events would correspond to the diffraction limited imaging properties of our instrument. We verified the resolution of our confocal instrument to be diffraction limited using fluorescent beads (~200 nm in diameter). The recorded point spread function had an FWHM of 390 nm × 390 nm × 1000 nm for the *x*-, *y*- and *z*-directions, corresponding to a volume of ~0·12 μm^3.

Flash photolysis

A xenon short-arc flash lamp (maximum output, 230 J; duration of flash, ~0·6 ms) was used to photolyse DM-nitrophen in an epi-illumination arrangement (Lipp *et al.* 1996). Wavelengths between 340 and 390 nm were passed through a liquid light guide into the fluorescence port of an inverted microscope (Nikon Diaphot). After reflection by a dichroic mirror the light passed the objective (Neofluar ×63; NA, 1·25; Zeiss) and homogeneously epi-illuminated the entire field. Upon flash photolysis of DM-nitrophen, Ca^{2+} was released rapidly with a half-time of ~30 μs (Escobar, Cifuentes & Vergara, 1995). The flash intensity was varied by changing the energy stored in the capacitors. To avoid artefacts in the fluorescence records, flashes were triggered during retrace of the laser scan.

RESULTS

A comparison between a Ca^{2+} transient triggered by an L-type Ca^{2+} current and a Ca^{2+} signal resulting from a UV flash (75 J discharged energy) is shown in Fig. 1. Line-scan images of a cell loaded with the Ca^{2+}-sensitive fluorescent dye fluo-3 were acquired by rapidly and repeatedly scanning a single line of a confocal optical section. The recorded lines were then arranged from left to right to form line-scan images that contain information about the amplitude of the Ca^{2+} signals (pseudocolour) *versus* time, but also reveal spatial information in one dimension (represented vertically). A small L-type Ca^{2+} current of about 20 pA (in the presence of 10 μM verapamil; Fig. 1*A*) resulted in numerous spatially localized and short-lived Ca^{2+} signals with properties very similar to the spontaneous Ca^{2+} sparks mentioned above (width at half-maximal amplitude, 1·65 μm; amplitude, 250 nM; rapid decay, with a time constant of ~60 ms due to diffusion of Ca^{2+} away from the volume governed by the spark). In

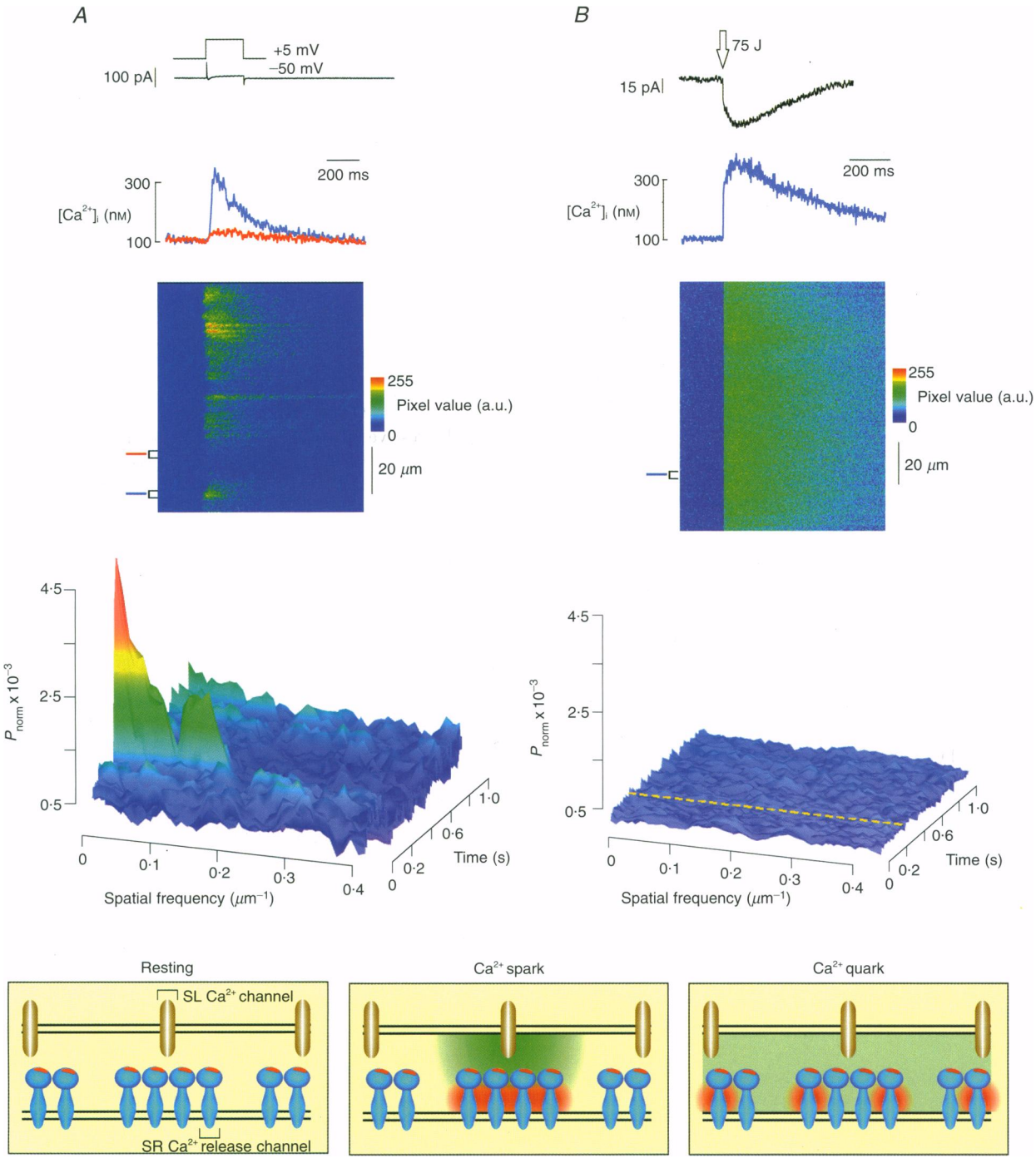

Fig. 1. Comparison of a Ca^{2+} transient induced by I_{Ca} and by a photochemical Ca^{2+} jump in the same cell

A, a voltage-clamp depolarization from −50 to +5 mV activated a small I_{Ca} due to a partial block by submaximal concentration of verapamil (10 μM). The line-scan image reveals several localized Ca^{2+} signals. These Ca^{2+} sparks rose to 350 nM (blue trace) while the changes of $[Ca^{2+}]_i$ in regions between sparks were limited to ~25 nM (red trace). The power spectra in the spatial domain exhibited a pronounced burst of low frequencies characteristic for localized Ca^{2+} signals. *B*, later during the experiment a flash was applied at the fixed holding potential of −50 mV resulting in an inwardly directed membrane current (50 pA) due to Ca^{2+} removal via Na^+–Ca^{2+} exchange (I_{Na-Ca}). The Ca^{2+} trace (blue) suggests a Ca^{2+} jump to 375 nM and the line-scan image reveals no spatial non-uniformities. This is confirmed in the flat power spectra. Note that power units are arbitrary but identical in all spectra shown in this paper, and time runs from front to back. The yellow dashed line indicates the moment of flash. *C*, diagram of a possible microarchitecture for the SL–SR junction with individual SL Ca^{2+} channels facing a cluster of SR Ca^{2+} release channels in a cleft that is ~20 nm wide. Ca^{2+} entering via an SL Ca^{2+} channel forms a domain of elevated Ca^{2+} (green) that is 'seen' by a possible Ca^{2+} binding site on the SR Ca^{2+} release channels (red spot with preferential access for Ca^{2+} entering via SL Ca^{2+} channel). This trigger signal activates all Ca^{2+} release channels within a cluster, giving rise to a Ca^{2+} spark. Photochemical Ca^{2+} release is homogeneous (green haze) and can recruit individual SR Ca^{2+} release channels from within various clusters, giving rise to several Ca^{2+} quarks.

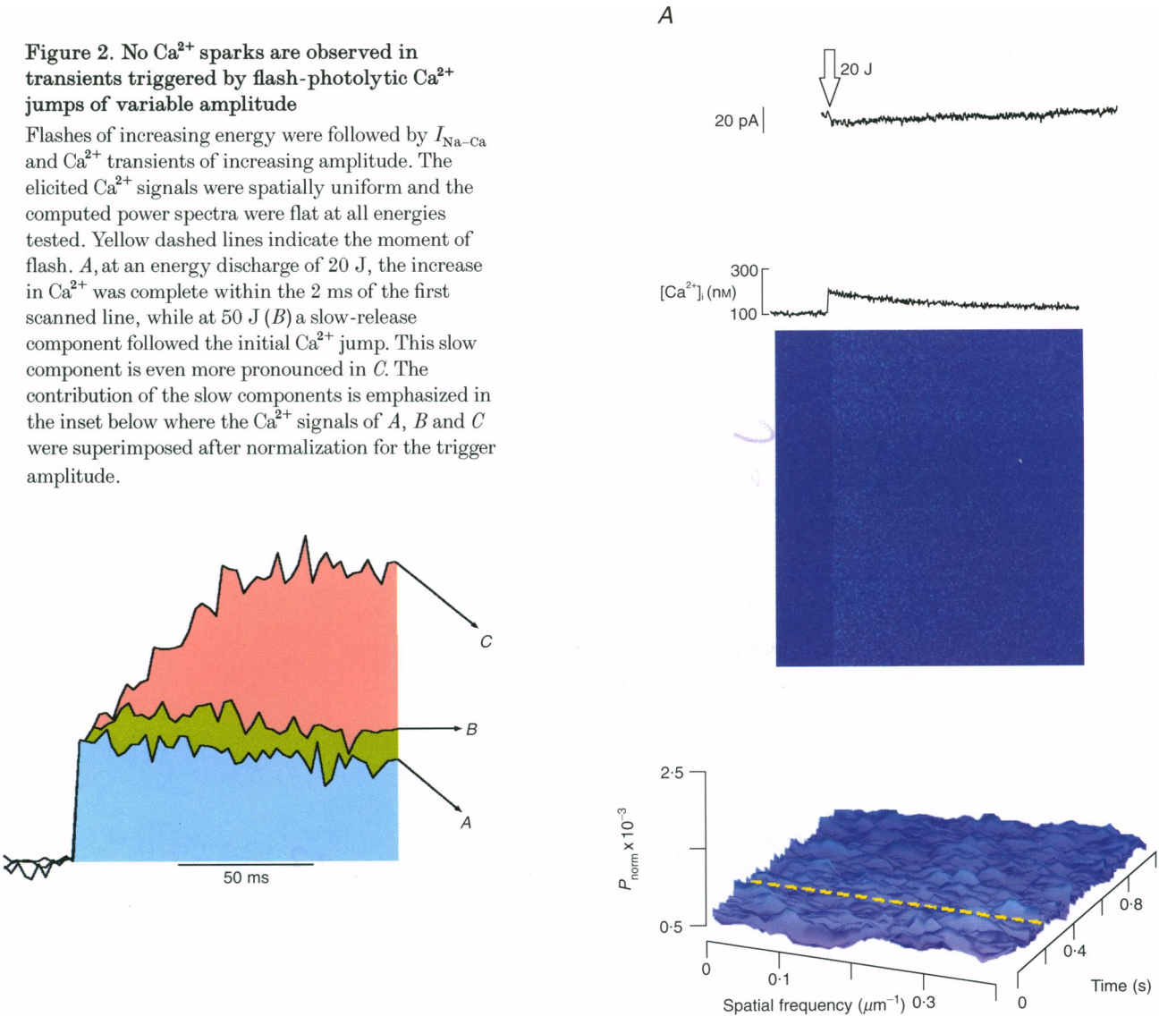

Figure 2. No Ca^{2+} sparks are observed in transients triggered by flash-photolytic Ca^{2+} jumps of variable amplitude

Flashes of increasing energy were followed by I_{Na-Ca} and Ca^{2+} transients of increasing amplitude. The elicited Ca^{2+} signals were spatially uniform and the computed power spectra were flat at all energies tested. Yellow dashed lines indicate the moment of flash. *A*, at an energy discharge of 20 J, the increase in Ca^{2+} was complete within the 2 ms of the first scanned line, while at 50 J (*B*) a slow-release component followed the initial Ca^{2+} jump. This slow component is even more pronounced in *C*. The contribution of the slow components is emphasized in the inset below where the Ca^{2+} signals of *A*, *B* and *C* were superimposed after normalization for the trigger amplitude.

contrast, the flash-photolytically generated Ca^{2+} transient of similar peak amplitude (275 nM) appeared to be spatially uniform and exhibited a slower decay, with a time constant of 560 ms, presumably because there was no concentration gradient to neighbouring cytosolic spaces (Fig. 1*B*). This impression was also confirmed with a power spectral analysis of the line-scans depicted in the bottom panels in Fig. 1. The power spectra were computed with a fast Fourier transform (FFT) algorithm from the line-scan image in the spatial domain (i.e. in the vertical direction).

A surge of spatial low-frequency components between 0·01 and 0·13 μm^{-1} was present in the Ca^{2+} transient triggered by openings of SL Ca^{2+} channels. In contrast, the spectrum of the flash photolytic Ca^{2+} signal did not exhibit significant power peaks. The absence of localized and rapidly decaying Ca^{2+} signalling events and the lack of low-frequency components in the power spectra suggest that the photolytic Ca^{2+} trigger did not elicit Ca^{2+} sparks. How can this surprising finding be explained? At least three possibilities are conceivable. (i) The flash-induced Ca^{2+} jump may be too small to trigger Ca^{2+} release from the SR and we are only recording the photolytic Ca^{2+} signal. (ii) The photochemical Ca^{2+} jump after the flash may be so large that it overwhelms the cell with Ca^{2+} and thus engulfs the Ca^{2+} sparks. (iii) The real elementary SR Ca^{2+} release events triggered by photorelease of Ca^{2+} may be considerably smaller in size and/or amplitude than a Ca^{2+} spark. The third possibility is highly interesting and would challenge present models of E–C coupling and cardiac Ca^{2+} signalling (Fig. 1*C*). We pursued two experimental strategies to discriminate among these possibilities.

Ca^{2+} sparks can more easily be detected in line-scans when their number is fairly small. Photolytic triggers slightly above the threshold for SR Ca^{2+} release would be predicted to activate only a few release units and thus to reveal Ca^{2+} sparks. Therefore, photolysis experiments were performed at various flash energies. Figure 2 summarizes these results and shows that the Ca^{2+} signals and the SR Ca^{2+} release were graded and correlated with the flash energy used. However, changing the energy did not reveal spatial

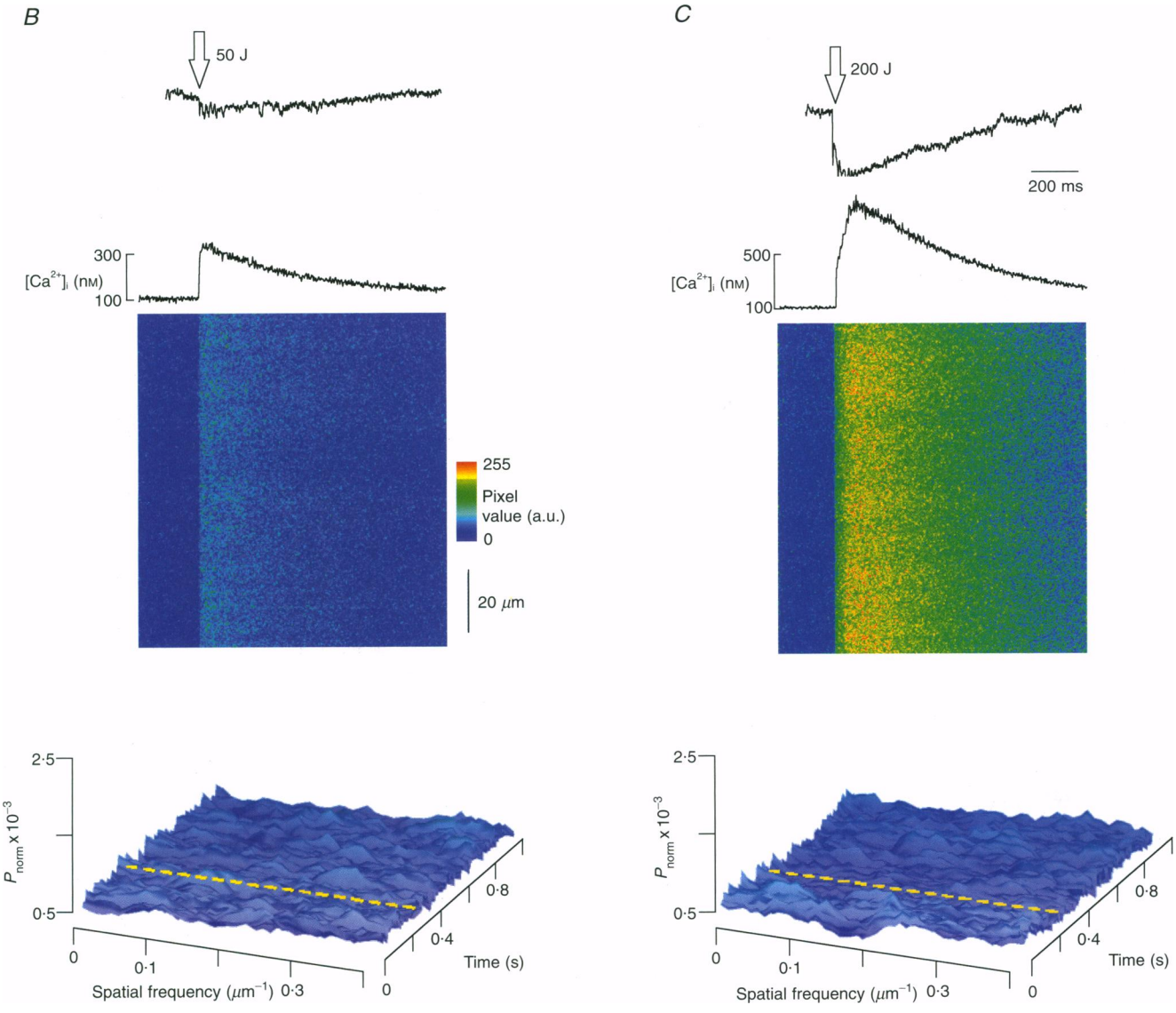

inhomogeneities (i.e. Ca^{2+} sparks) as can be verified in the power spectra computed for each energy level. Differences in the time course of these Ca^{2+} transients provide evidence that the photolytic Ca^{2+} jump was indeed above trigger threshold at 50 and 200 J but below threshold at 20 J. A discharged energy of 20 J instantaneously (i.e. within the 2 ms sampling interval) elevated the Ca^{2+} concentration from 100 to 200 nM and was followed by a monotonic decay of $[Ca^{2+}]_i$. Increasing the flash energy to 50 J again produced an instantaneous Ca^{2+} jump (to 300 nM) but was succeeded by a distinctive but slower phase of rising $[Ca^{2+}]_i$ resulting from CICR and peaking at 340 nM after 22 ms. When the flash energy was raised further to 200 J, the rapid Ca^{2+} jump to 390 nM triggered substantial additional SR Ca^{2+} release which reached 930 nM after 90 ms. In addition, the slow component in the Ca^{2+} transients was abolished when the myocytes were pre-incubated in 20 μM ryanodine (not shown). The two phases visible in the time course of the Ca^{2+} signals allow a rough assessment of the 'apparent amplification' by CICR: 0% for 20 J, 20% for 50 J and 186% for 200 J. This estimate of the 'apparent amplification' of CICR is crude, since we cannot temporally separate the two components in a reliable way because CICR has presumably already started during the photochemical Ca^{2+} release. Accordingly, the three records represent photolytic trigger experiments performed below threshold, slightly above and well above threshold for CICR. Taken together, these results indicate that Ca^{2+} sparks were not elicited by flash photolysis of caged Ca^{2+} independent of the energy discharged ($n = 45$ flashes in 5 cells). Instead, flash photolysis seemed to trigger Ca^{2+} release units that were substantially smaller in size or amplitude than Ca^{2+} sparks.

Since the range for near-threshold photolytic Ca^{2+} concentration jumps may be very narrow and may depend on variabilities of SR Ca^{2+} loading, we devised a method of directly visualizing the threshold of SR Ca^{2+} release. By applying a continuous gradient of flash energy across the cell it was possible to dissect spatially sub- and supra-threshold Ca^{2+} jumps (Fig. 3). This experimental approach

resulted in a clearly distinguishable point along the scanned line reflecting the apparent threshold concentration for SR Ca^{2+} release (~350 nM in this particular cell). The precise trigger threshold cannot be determined because fluo-3 may not be kinetically fast enough to follow the real $[Ca^{2+}]_i$ (Escobar *et al.* 1995). Above this point, the photolytic Ca^{2+} jump was suprathreshold; below this point only the photochemical signal was elicited, visible as a pedestal in the surface plot of $[Ca^{2+}]_i$ derived from the line-scan image (Fig. 3*B*). Interestingly, a Ca^{2+} wave was initiated by the SR Ca^{2+} release that propagated into the cellular region where the

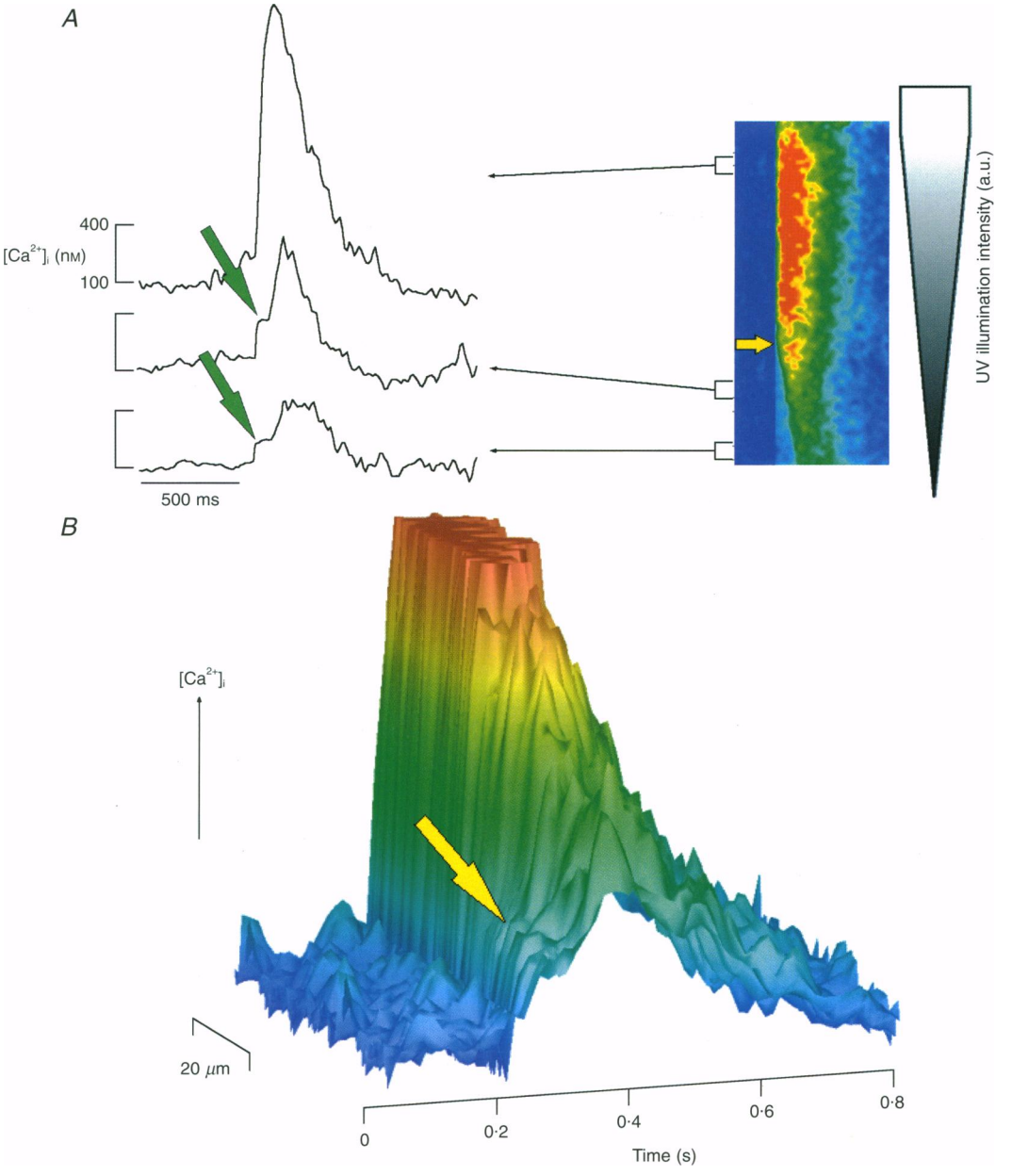

Figure 3. Sub- and suprathreshold Ca^{2+} release generated by a gradient of flash energy across the cell

A, a ratiometrically calibrated fluo-3–fura-red line-scan during application of a flash encompassing an energy gradient. The colour look-up table was transformed and adjusted to emphasize the apparent threshold point for CICR (yellow arrow). Local Ca^{2+} transients from three subcellular regions are shown as line-plots. The green arrows point to the photolytic Ca^{2+} triggers in the subthreshold part of the cell. *B*, a photolytic Ca^{2+} trigger that was subthreshold for SR Ca^{2+} release can be seen as a pedestal (arrow) in this surface plot computed from the processed line-scan image in *A*.

photolytic trigger was below threshold. The propagating wave confirms that CICR in this region below the apparent threshold was potentially excitable and that the initial failure of CICR was not due to an obstacle (e.g. the cell nucleus). Although the trigger signal obviously encompassed all possible near-threshold Ca^{2+} concentrations in such experiments ($n = 8$ flashes in 3 cells), no sparks were detected in the line-scan images. In addition, power spectra performed on a cell region located in the vicinity of the threshold point were flat (not shown).

DISCUSSION

The most important conclusion from these results is that the fundamental event of Ca^{2+} signalling, as triggered by flash photolysis of caged Ca^{2+}, has to be considerably smaller than a Ca^{2+} spark. We therefore refer to this fundamental event as a Ca^{2+} 'quark' possibly reflecting gating of a single SR Ca^{2+} release channel. How can we fit Ca^{2+} quarks and Ca^{2+} sparks together? This inevitably requires an extension of the 'spark hypothesis' for cardiac Ca^{2+} signalling proposed recently and outlined above (Cheng *et al.* 1993; Niggli & Lipp, 1995). Our findings are consistent with the view that Ca^{2+} sparks represent elementary events in cardiac Ca^{2+} signalling, but only for signals mediated by SL Ca^{2+} channels or during spontaneous SR Ca^{2+} release under conditions of relatively high SR Ca^{2+} load. In both cases a group of SR Ca^{2+} release channels may be activated in an all-or-none fashion to form a Ca^{2+} spark because (i) the trigger signal via the SL Ca^{2+} channel is large and saturates all SR Ca^{2+} release channels within a group, possibly by preferential access to binding sites for Ca^{2+}, or (ii) because the positive feedback in the CICR is fairly high, perhaps due to the SR Ca^{2+} load (Trafford, O'Neill & Eisner, 1993). Both conditions would favour spread of the Ca^{2+} signal within such a group of SR Ca^{2+} release channels and thus lead to all-or-none behaviour, i.e. Ca^{2+} sparks (see Fig. 1*C*). Although our results are also consistent with a homogeneous distribution of the Ca^{2+} release channels, the functional scheme with clusters has the advantage of easily explaining why spontaneous and triggered sparks appear to have the same size and amplitude (Niggli & Lipp, 1992; Cheng *et al.* 1993). Furthermore, it could readily be reconciled with some morphological clustering of SR Ca^{2+} release channels, either as a complete diad or a subset of channels within a T-tubule–SR junction. In skeletal muscle such an ultrastructural arrangement has indeed been reported (Block, Imagawa, Campbell & Franzini-Armstrong, 1988), but morphological information for mammalian cardiac muscle on this level is still lacking.

Another significant result of this paper is that individual fundamental Ca^{2+} release units (presumably SR Ca^{2+} channels) within such clusters can be recruited by a homogeneous trigger (e.g. a photochemical Ca^{2+} jump; see Fig. 1*C*). In this regard, it is important to realize that the volume governed by a spark may contain a large number SR Ca^{2+} release channels. A substantial difference between I_{Ca}-induced CICR and photolytically activated CICR is expected to arise from the notably dissimilar spatial properties of the two Ca^{2+} triggers. While the Ca^{2+} influx via SL Ca^{2+} channels is believed to result in a steep concentration gradient around the inner opening of the channel, flash photolysis elevates Ca^{2+} in a spatially homogeneous manner, presumably even on a submicroscopic scale. In the presence of 20 μM ryanodine (i.e. without SR Ca^{2+} release), the Ca^{2+} transients were always homogeneous at the spatial resolution given by the confocal microscope and had flat power spectra (not shown). Submicroscopic concentration gradients have been implicated in the local control mechanism, but the spatially homogeneous flash-photolytic trigger activates SR Ca^{2+} release channels without being subject to local control requiring the interaction between SL Ca^{2+} channels and SR Ca^{2+} release channels. This implies that the all-or-none behaviour of such a group, although evident as Ca^{2+} sparks, is not an intrinsic property of these clusters but may depend on the degree of positive feedback in the system and/or on the amplitude of the trigger (Niggli & Lederer, 1990; Stern, 1992). Therefore, Ca^{2+} quarks presumably also contribute to the signal amplification during E–C coupling but simply escape confocal microscopic detection because of their limited amplitude or size. In addition, SR Ca^{2+} release triggered by I_{Na} was also always spatially homogeneous and exhibited flat power spectra (Lipp & Niggli, 1994*a*). This type of Ca^{2+} signalling is assumed to activate preferentially junctional SR Ca^{2+} release channels via Ca^{2+} influx mediated by Na^+–Ca^{2+} exchange. Therefore, this observation indicates that the homogeneous Ca^{2+} release observed after flash photolysis reflects a property of the trigger signal (i.e. homogeneous *versus* localized trigger) and does not result from the recruitment of SR compartments other than junctional ones (e.g. corbular).

Simulations of Ca^{2+} diffusion in the narrow junctional cleft between SL and SR were performed with computer models developed by us. These results indicate that, contrary to the situation in a hemisphere, a steady-state [Ca^{2+}] profile is not reached within microseconds of the opening of an SL Ca^{2+} channel. Instead $[Ca^{2+}]_i$ continues to rise during the channel opening (Amstutz, Michailova & Niggli, 1996). Therefore, it is conceivable that short SL Ca^{2+} channel openings can induce Ca^{2+} quarks but are not sufficient to evoke Ca^{2+} sparks.

Cardiac myocytes thus appear to implement a hierarchical Ca^{2+} signalling concept, with Ca^{2+} quarks as fundamental release elements. This design allows for multiple regulatory and modulatory mechanisms on distinct molecular, subcellular and cellular levels. Similar hierarchical concepts may exist in other cell types relying on spatially and temporally complex Ca^{2+} signalling systems (e.g. Tsugorka, Rios & Blatter, 1995).

AMSTUTZ, C., MICHAILOVA, A. & NIGGLI, E. (1996). The role of local events and diffusion in cardiac EC-coupling. *Biophysical Journal* **70**, A274.

BLOCK, B. A., IMAGAWA, T., CAMPBELL, K. P. & FRANZINI-ARMSTRONG, C. (1988). Structural evidence for direct interaction between the molecular components of the transverse tubule/sarcoplasmic reticulum junction in skeletal muscle. *Journal of Cell Biology* **107**, 2587–2600.

CANNELL, M. B., CHENG, H. & LEDERER, W. J. (1994). Spatial non-uniformities in $[Ca^{2+}]_i$ during excitation-contraction coupling in cardiac myocytes. *Biophysical Journal* **67**, 1942–1956.

CHENG, H., LEDERER, W. J. & CANNELL, M. B. (1993). Calcium sparks – elementary events underlying excitation-contraction coupling in heart muscle. *Science* **262**, 740–744.

ESCOBAR, A. L., CIFUENTES, F. & VERGARA, J. L. (1995). Detection of Ca^{2+}-transients elicited by flash photolysis of DM-nitrophen with a fast calcium indicator. *FEBS Letters* **364**, 335–341.

FABIATO, A. (1985). Time and calcium dependence of activation and inactivation of calcium-induced release of calcium from the sarcoplasmic reticulum of a skinned cardiac Purkinje cell. *Journal of General Physiology* **85**, 291–320.

HERMSMEYER, K., MASON, R., PUGA, A. & ERNE P. (1991). Subcellular localization of calcium release in isolated rat myocardial cells. *Journal of Cardiovascular Pharmacology* **18**, S23–35.

LIPP, P., LÜSCHER, C. & NIGGLI, E. (1996). Photolysis of caged compounds characterized by ratiometric confocal microscopy: A new approach to homogeneously control and measure the calcium concentration in cardiac myocytes. *Cell Calcium* (in the Press).

LIPP, P. & NIGGLI, E. (1994*a*). Sodium current-induced calcium signals in isolated guinea-pig ventricular myocytes. *Journal of Physiology* **474**, 439–446.

LIPP, P. & NIGGLI, E. (1994*b*). Modulation of Ca^{2+} release in cultured neonatal rat cardiac myocytes – insight from subcellular release patterns revealed by confocal microscopy. *Circulation Research* **74**, 979–990.

LÓPEZ-LÓPEZ, J. R., SHACKLOCK, P. S., BALKE, C. W. & WIER, W. G. (1995). Local calcium transients triggered by single L-type calcium channel currents in cardiac cells. *Science* **268**, 1042–1045.

NÄBAUER, M., CALLEWAERT, G., CLEEMANN L. & MORAD, M. (1989). Regulation of calcium release is gated by calcium current, not gating charge, in cardiac myocytes. *Science* **244**, 800–803.

NIGGLI, E. & LEDERER, W. J. (1990). Voltage-independent calcium release in heart muscle. *Science* **250**, 565–568.

NIGGLI, E. & LIPP, P. (1992). Spatially restricted Ca^{2+}-release in cardiac myocytes revealed by confocal microscopy. *Pflügers Archiv* **420**, suppl. 1, R81.

NIGGLI, E. & LIPP, P. (1995). Subcellular features of calcium signalling in heart muscle: what do we learn? *Cardiovascular Research* **29**, 441–448.

STERN, M. D. (1992). Theory of excitation-contraction coupling in cardiac muscle. *Biophysical Journal* **63**, 497–517.

TRAFFORD, A. W., O'NEILL, S. C. & EISNER, D. A. (1993). Factors affecting the propagation of locally activated systolic Ca transients in rat ventricular myocytes. *Pflügers Archiv* **425**, 181–183.

TSUGORKA, A., RIOS, E. & BLATTER, L. A. (1995). Imaging elementary events of calcium release in skeletal muscle cells. *Science* **269**, 1723–1726.

VALDIVIA, H. H., KAPLAN, J. H., ELLIS-DAVIES, G. C. R. & LEDERER, W. J. (1995). Rapid adaptation of cardiac ryanodine receptors: modulation by Mg^{2+} and phosphorylation. *Science* **267**, 1997–2000.

WIER, W. G., CANNELL, M. B., BERLIN, J. R., MARBAN, E. & LEDERER, W. J. (1987). Cellular and subcellular heterogeneity of $[Ca^{2+}]_i$ in single heart cells revealed by fura-2. *Science* **235**, 325–328.

Acknowledgements

We thank Drs H. P. Clamann, C. Lüscher, H.-R. Lüscher, S. Rohr and B. Schwaller for helpful comments on the manuscript and C. Amstutz and A. Michailova for discussions. This work was supported by a grant from the Swiss National Science Foundation (31.37417.93).

Received 7 December 1995; accepted 23 January 1996.